N87-22347

MEASUREMENTS OF ATMOSPHERIC TURBULENCE

Harold N. Murrow
NASA Langley Research Center
Hampton, Virginia

This paper is intended to address various types of atmospheric turbulence measurements for the purpose of stimulating discussion during the interactive committee sessions of the workshop where measurement requirements relative to available data may be addressed. An outline of these various types of measurements is as follows:

1. Characterization studies
   a. Integral scale value
   b. Spanwise gradient

2. Encounter studies
   a. Velocity, vertical acceleration in g's, and pressure altitude
   b. Special encounters

3. Other
   a. Ground-based measurement
   b. Other in situ measurements

4. Summary

Some specific results of detailed characterization studies made at NASA Langley will be emphasized. References [1] through [13] are pertinent to these measurements and some modeling studies associated with them. Reference will be made to an existing program for measuring the spanwise gradient of gust velocity [14-17]. The most recent reports on statistics of turbulence encounters for various types of aircraft operations are summarized [18,19]. Special severe encounter studies [20] and reference to remote sensing [21] are also included. Wind shear is considered to be a special topic and is not covered here.

The objectives of the NASA Measurement of Atmospheric Turbulence (MAT) program are to obtain atmospheric turbulence power spectra and determine appropriate values of the integral scale length, L, for different meteorological conditions (jet stream, low altitude clear air, mountain waves, and near thunderstorms) over an altitude range from near sea level to about 65,000 feet. The same instrumentation system and data reduction procedure was to be utilized for all measurements. Very low frequency measurements were required since the emphasis was on the long wavelength portion of the power spectrum in order to estimate values of L.

The classical von Karman expression is given in Figure 1 and shows that two parameters are required to describe a power spectrum, σ, the intensity, and L, the scale of the turbulence sample. The family of curves shown is normalized with respect to intensity and shows how the location of the "knee" or flattening of the power spectrum changes with L. Some design

specifications designate that L = 2500 ft be utilized if power spectral analysis techniques are to be used.

As shown in Figure 2, the gust characteristics of most contemporary aircraft are in a frequency range that knowledge of an appropriate L value is not needed; however, for large flexible supersonic aircraft, the principal response is at much lower frequencies. Thus, the aircraft response can be significantly different for the same intensity turbulence (note the log scales on the figure), and utilization of an appropriate L for design is important.

An instrumented B-57B Canberra aircraft was utilized as the sampling airplane. Samples of clear-air turbulence were obtained for conditions shown in Figure 3. While the instrumentation was later installed on a B-57F for higher altitude samplings, due to various difficulties, data sufficient for publication was not acquired.

The equations in Figure 4 show how the primary measurements made by balsa flow vanes and a sensitive airspeed device were corrected by use of instrumentation that measured aircraft motion to result in three components of gust velocity, longitudinal, lateral, and vertical with respect to the sampling aircraft.

Figures 5 through 8 give example true gust velocity time histories measured under different meteorological conditions. Four cases were selected by a research meteorologist as representing turbulence caused by low-altitude convective activity, mountain wave action, high-altitude wind shear, and so-called rotor action with sampling in the lee of rather sharp mountain peaks in the presence of strong wind. The convective case shown in Figure 5a resulted from a run extending for approximately 150 miles at 1000 ft altitude near the Virginia and North Carolina line and exhibits similar characteristics for all three components, and their σ values ranged from 3.78 to 4.41 ft/sec.

In Figure 5b the shape of the spectra for the convective case is reasonably close to the von Karman representation (shown by the solid lines superimposed on the data curves); however, in order to have a reasonable fit, L values of 1000, 2000, and 4000 ft appear appropriate for the vertical, lateral, and longitudinal components, respectively.

Time histories for the mountain wave case shown in Figure 6a are distinctively different in that major long wavelength content is obvious. At least three wave cycles are obvious in the 12-minute run for the vertical component--approximately one longer wave is noted on the horizontal components. The high-frequency content is variable in intensity and for this and other mountain wave samples it appears to intensify during positive swings in vertical gust velocity.

In Figure 6b the power spectra for the mountain wave case emphasize the observations noted on the time histories. High power is evident at long wavelengths and fitting a von Karman representation to the data is very difficult. It should also be noted that the higher frequency data exhibit the expected 5/3 slope, then tend to flatten, and then rise sharply in power at lower frequencies.

Observation of time histories shown in Figure 7a indicate that the wind shear case characteristics, in general, seem to fit between the convective and mountain wave cases with intensity varying gradually with time. It is known that this nonhomogeneous or nonstationary behavior will affect the "knee" of the corresponding power spectrum. An assessment of this effect will be shown later.

The power spectra for the wind shear case shown in Figure 7b indicate more power content in the horizontal components at low frequencies than the vertical component and less severe. The von Karman model can be made to fit reasonably well, especially for the vertical component. Appropriate integral scale values are in the range of 6000 ft for the horizontal components and 1000 ft for the vertical component.

The time histories for the rotor case shown in Figure 8a exhibit continual high-intensity, high-frequency turbulence and some long wavelength content is obviously included. The standard deviation, σ, for the vertical gust velocity component is 12.5 ft/sec--more than 50 percent greater than any other sample acquired. Acceleration increments of 1 g were equaled or exceeded 80 times in this traverse with maximum incremental accelerations of +2.2 g and -1.8 g.

The power spectra for the rotor case are shown in Figure 8b. It appears that an integral scale value of 6000 ft for the von Karman expression would approximate the spectra reasonably well.

Table 1 summarizes the four cases shown in Figures 5 through 8 with respect to altitude, length of run (in both time and miles), statistical degrees of freedom applicable for the power spectra, and values of standard deviation for the three gust velocity components.

The results of Figure 9 were obtained in an analytical study by Dr. William Mark of Bolt, Beranek, and Newman and provide "rule of thumb" guidance on the effects of intensity variation on the resulting power spectrum. Here, L_σ, is the spatial length of the sampling run for a linear increase and one half of the spatial length for an intensity burst, and L is the integral scale value of the turbulence. For the ratio of L_σ/L greater than 10 to 13, the effect on the power spectrum is barely detectable whereas for ratios below 5 to 7 a strongly rounding effect will be present.

Figure 10 summarizes the approximate relative integral scale values for the four cases. Because the turbulence in the mountain wave case is not continuous, the use of power spectra for characterization is somewhat questionable.

The objectives of the sampling program with the additional probes at the wing tips are given on Figure 11. It is interesting to note that whereas the emphasis in the MAT program was on the low-frequency portion of the power spectrum, the emphasis here is at the higher frequencies.

The B-57B was again utilized as the sampling test bed. The aircraft was selected because of its rugged design, broad flight envelope, ease of flying, and availability (see Figure 12). The wing tip probes located 60 feet apart are mounted at locations designed to accept fuel pods.

Figure 13 (taken from Houbolt and Sen [14]) shows theoretical prediction of the cross-spectra for the same gust component a distance S apart, assuming homogeneous isotropic turbulence. The curves are for various ratios of S/L where L is the integral scale value. Note that for $\sigma = S/L = 0$, the curve would be a von Karman spectrum with a -5/3 slope at higher frequencies. Flights are being made at low altitude where L is expected to be small and thus get an expected deviation from S/L = 0, and this region is appropriate since the spanwise effects are especially important for pilot workload in the terminal area.

Figure 14 shows some example time histories from the two wing tips and the centerline. While the general and long wavelength characteristics are similar, significant differences are evident in the mid and higher frequency region.

Figure 15a shows the auto-power spectra (APSD) for each wing tip with a fitted von Karman spectrum superimposed on the measured data. The L value from the fitted spectrum is used to provide the theoretical curve for cross-spectra (labeled CPSD) on Figure 15b. An example case of flight data is also shown. In this case the data deviate further from the prediction at the higher frequencies. The effects of filtering and data processing are presently under study.

Significant research and development efforts are under way in the remote sensing area. The use of Doppler radar and lidar (light detection and ranging) is encouraging. Some example data are shown in Figure 16 (from [21]) where power spectral estimates from ground-based lidar, in situ aircraft measurements, and tower measurements are shown. Lidar data are shown up to a frequency of 1 Hz; however, the agreement deteriorates above about 0.1 Hz. The authors of Reference [21] attribute this to a decrease in signal-to-noise ratio for the lidar data. The development and application of airborne units is expected to expand in the near future.

Figure 17 gives a summary of the NASA VG (velocity, vertical acceleration in g's) and VGH (velocity, vertical acceleration in g's, and pressure altitude) program. This program was a continuing effort to obtain pertinent statistical information on transport aircraft turbulence encounters. Recorders were installed on many aircraft over a 20-year period. From time history records of indicated airspeed, pressure altitude, and normal acceleration, peak values of derived gust velocity were determined. This program has been terminated, and the last report was published in 1977. A general aviation program was conducted in the 1960 to 1982 time period where various operation types were studied. Data were obtained for a total of 42,155 hours from 105 airplanes. Reporting is nearly complete.

The feasibility of utilizing data available from transport crash recorders to provide VGH-type information has been demonstrated and is outlined in Figure 18. In addition, an instrument has been developed that can record, store, and provide statistical data in a desired format. At the present time, there is no on-going activity in these areas.

Special analyses are being conducted of severe turbulence encounters utilizing data from on-board flight data recorders. A summary of these

analyses is given in Figure 19. The procedure, which is shown on Figure 20, involves applying measured inertial and air data to equations of motion with parametric values appropriate for the particular aircraft involved. The derived atmospheric disturbance data can then be installed on a simulator for study of response of various aircraft to that disturbance. Figure 20 gives a block diagram of the analysis procedure and lists cases of wide-body special severe encounters for which data are presently available.

Results to date for several high-altitude cases indicate that a strong shear layer has been destabilized either by storm passage or mountain waves. For these cases, the disturbance is not of continuous random nature but periodic large vortex flows.

To summarize the status of measurement of atmospheric turbulence, it appears that no new measurements for characterization of clear-air turbulence are being planned; however, measurements--perhaps with less severe requirements--are being made to support other atmospheric measurement programs. The VGH work is inactive; however, if funding were available, a new recorder could be utilized that would greatly simplify the process of converting the data to publication form. Remote sensing developments are expected to continue and results to date are encouraging. A better understanding of unexpected high-altitude encounters should result from incident studies utilizing on-board recorder information, and results from this, spanwise gradient measurements and others should lead to more realistic simulation work.

It is expected that turbulence measurements will continue to be made in the future to support further developments in forecasting, development of detection devices, and evaluate design techniques and the validation of gust alleviation systems.

References

Measurement:

1. Murrow, H. N.; and Rhyne, R. H.: The MAT Project--Atmospheric Turbulence Measurements with Emphasis on Long Wavelengths. Proceedings of the Sixth Conference on Aerospace and Aeronautical Meteorology of the American Meteorological Society, Nov. 1974, pp. 313-316.

2. Rhyne, R. H.; Murrow, H. N.; and Sidwell, K.: Atmospheric Turbulence Power Spectral Measurements to Long Wavelengths for Several Meteorological Conditions. Aircraft Safety and Operating Problems, NASA SP-416, 1976, pp. 271-286.

3. Murrow, H. N.; McCain, W. E.; and Rhyne, R. H.: Power Spectral Measurements of Clear-Air Turbulence to Long Wavelengths for Altitudes Up to 14000 Meters. NASA TP-1979, 1982.

4. Davis, R. E.; Champine, R. A.; and Ehernberger, L. J.: Meteorological and Operation Aspects of 46 Clear Air Turbulence Sampling Missions With an Instrumented B-57B Aircraft, Volume I--Program Summary. NASA TM-80044, 1979.

5. Waco, D. E.: Meteorological and Operational Aspects of 46 Clear Air Turbulence Sampling Missions With an Instrumented B-57B Aircraft, Volume II (Appendix C)--Turbulence Missions. NASA TM-80045, 1979.

6. Waco, D. E.: Mesoscale Wind and Temperature Fields Related to an Occurrence of Moderate Turbulence Measured in the Stratosphere Above Death Valley. *Mon. Weather Rev.*, 106(6):850-858, June 1978.

Modeling:

7. Reeves, P. M.; Campbell, G. S.; Ganzer, V. M.; and Joppa, R. G.: Development and Application of a Non-Gaussian Atmospheric Turbulence Model for Use in Flight Simulators. NASA CR-2451, Sept. 1974.

8. Sidwell, K.: A Mathematical Study of a Random Process Proposed as an Atmospheric Turbulence Model. NASA CR-145200, 1977.

9. Sidwell, K.: A Qualitative Assessment of a Random Process Proposed as Atmospheric Turbulence Model. NASA CR-145247, 1977.

10. Mark, W. D.; and Fischer, R. W.: Investigation of the Effects of Nonhomogeneous (or Nonstationary) Behavior on the Spectra of Atmospheric Turbulence. NASA CR-2745, 1976.

11. Mark, W. D.: Characterization of NonGaussian Atmospheric Turbulence for Prediction of Aircraft Response Statistics. NASA CR-2913, 1977.

12. Mark, W. D.; and Fischer, R. W.: Statistics of Some Atmospheric Turbulence Records Relevant to Aircraft Response Calculations. NASA CR-3464, 1981.

13. Mark, W. D.: Characterization, Parameter Estimation, and Aircraft Response Statistics of Atmospheric Turbulence. NASA CR-3463, 1981.

Spanwise Gradient:

14. Houbolt, J. C.; and Sen, A.: Cross-Spectral Functions Based on von Karman's Spectral Equation. NASA CR-2011, 1972.

15. Camp, D.; Campbell, W.; Frost, W.; Murrow, H.; and Painter, W.: NASA's B-57B Gust Gradient Program. *AIAA Journal of Aircraft*, 21(3):175-182, March 1984.

16. Campbell, W.; Camp, D. W.; and Frost, W.: An Analysis of Spanwise Gust Gradient Data. *Preprints: 9th Conference on Aerospace and Aeronautical Meteorology*, June 6-9, 1983, Omaha, Neb., p. 7.

17. Painter, W. D.; and Camp, D. W.: NASA B-57B Severe Storms Flight Program. NASA TM-84921, 1983.

VGH:

18. Zalovcik, J. A.; Jewel, J. W., Jr.; and Morris, G. J.: Comparison of VGH Data from Wide-Body and Narrow-Body Long-Haul Turbine-Powered Transports. NASA TN D-8481, July 1977.

19. Jewel, J. W., Jr.: Tabulations of Recorded Gust and Maneuver Accelerations and Derived Gust Velocities for Airplanes in the NASA VGH General Aviation Program. NASA TM 84660, Sept. 1983.

Special Encounters:

20. Parks, E. K.; Wingrove, R. C.: Bach, R. E.; and Mehta, R. S.: Identification of Vortex-Induced Clear Air Turbulence Using Airline Flight Records. *AIAA Journal of Aircraft*, 22(2):124-129, Feb. 1985.

Lidar:

21. Frost, W.; Huang, K. H.; and Theon, J. S.: Comparison of Winds and Turbulence Measurement from Doppler Lidar and Instrumented Aircraft. Presented at the Third Topical Meeting on Coherent Laser Radar, Worcestershire, England, July 8-11, 1985.

QUESTION: George Treviño (Michigan Tech). I saw by your measurements that you had some different scale lengths for the longitudinal scales and the vertical scales (6000 ft versus 1000 ft). That to me would indicate a very strong anistropy in the turbulence but yet you got some very good correlation with the theoretical isotropic von Karman spectra. How do explain that? Some of the data indicate a strong anistropy but yet you do get correlation with an isotropic curve?

ANSWER: As I mentioned earlier, I think that comes about because of the very high power content at the very low frequencies which is down to where you have wind effects. The question is where does the turbulence end and the wind begin? The high power content can be seen in the horizontal components but not in the vertical components. That's true if you are talking about frequencies that go all the way down to those low values or out to those long wavelengths.

TABLE 1. Four Selected Cases.

Meteorological condition	Altitude, km (ft)	Run length		Statistical d. f. for power spectra	$\sigma_{w'}$ m/sec (ft/sec)	$\sigma_{v'}$ m/sec (ft/sec)	$\sigma_{u'}$ m/sec (ft/sec)
		min.	km (miles)				
Convective	0.3 (1000)	19.1	148 (91.7)	45	1.15 (3.78)	1.18 (3.86)	1.35 (4.41)
Wind shear	13.0 (42600)	12.2	137 (85.1)	29	2.45 (8.05)	7.33 (24.04)	4.48 (14.70)
Rotor	3.9 (12800)	8.1	88.5 (55.0)	19	3.82 (12.52)	5.51 (18.09)	3.57 (11.73)
Mountain wave	14.3 (46800)	12.6	149 (92.4)	29	1.34 (4.41)	5.39 (17.69)	4.30 (14.11)

d. f. = f(bandwidth, length)

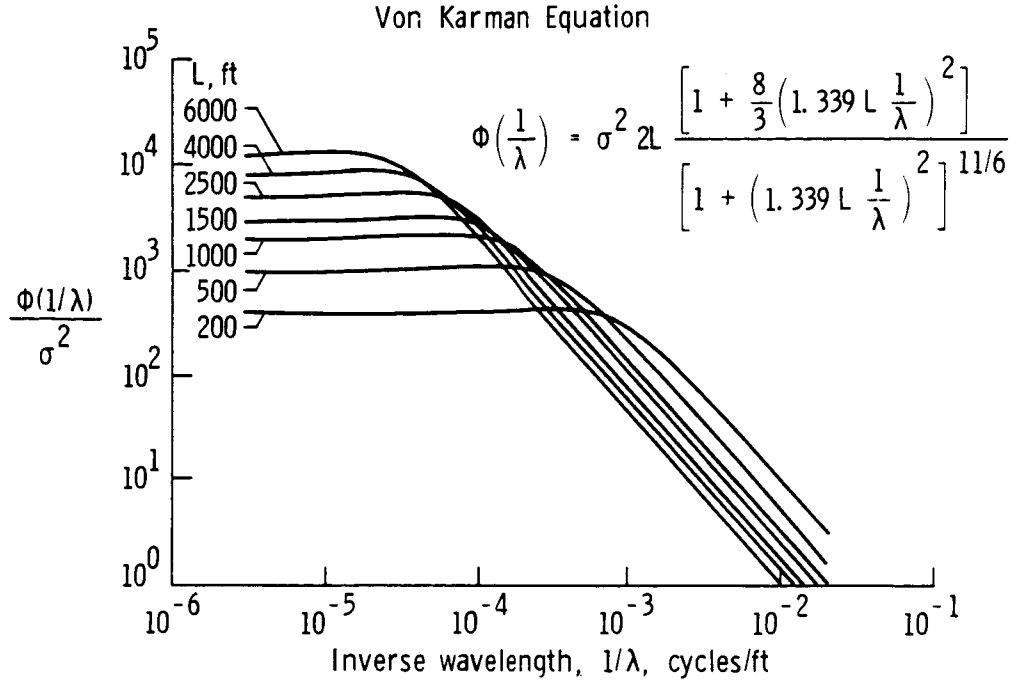

Figure 1. Theoretical transverse power spectra.

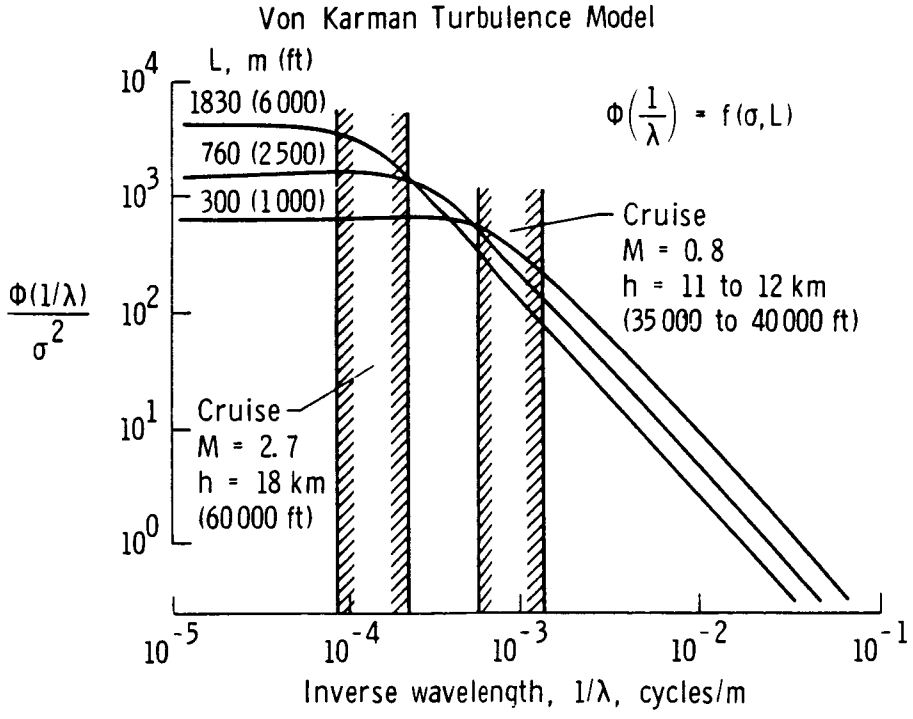

Figure 2. Theoretical power spectra.

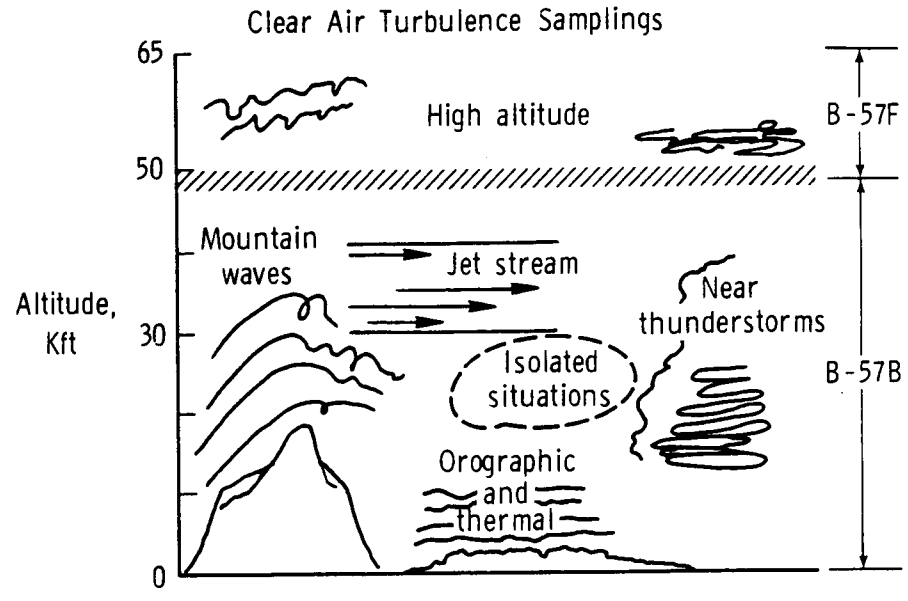

Figure 3. MAT project.

$$\text{Gust velocity component} = \left[\text{Primary measurement}\right] + \left[\text{Aircraft motion corrections}\right]$$

Longitudinal

$$u_g = [\Delta V] + \left[v_{ax} \sin \bar{\psi} + v_{ay} \cos \bar{\psi}\right]$$

Lateral

$$v_g = [V\beta] + \left[-V\Delta\psi + v_{ax} \cos \bar{\psi} - v_{ay} \sin \bar{\psi} + l\dot{\psi} + V\alpha\Phi\right]$$

Vertical

$$w_g = [V\alpha] + \left[-V\theta + v_{az} + l\dot{\theta} - V\beta\Phi\right]$$

Figure 4. Equations for the determination of gust velocity component time histories.

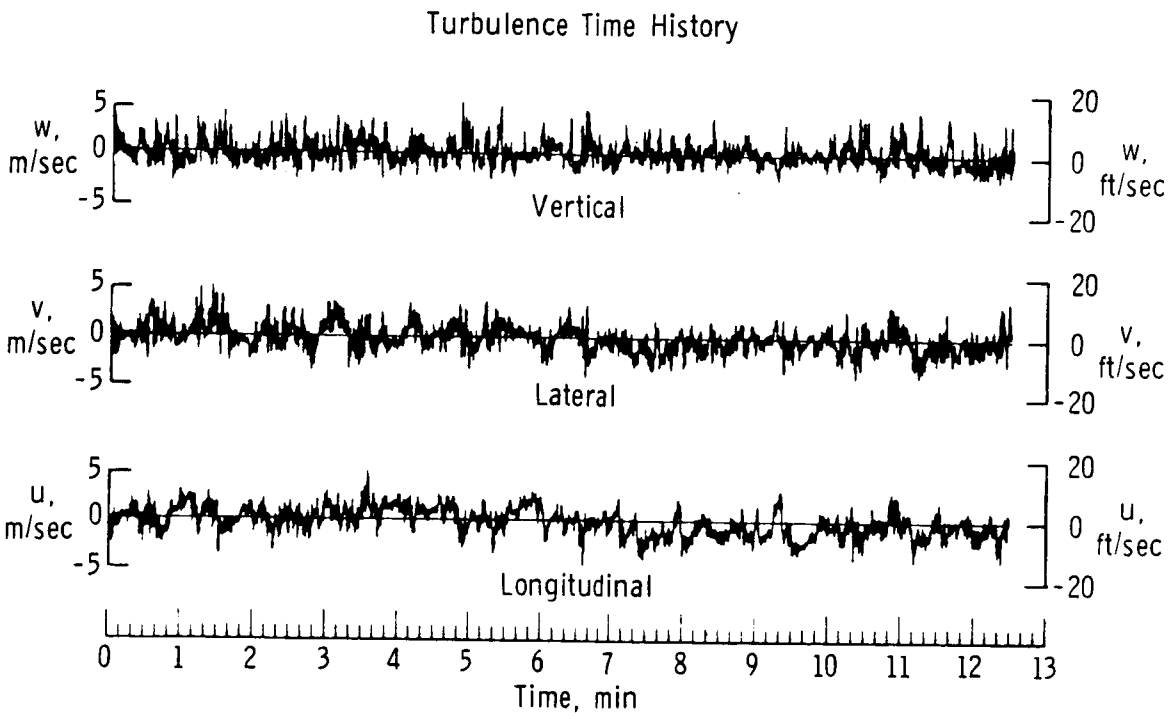

(a) Turbulence time history.

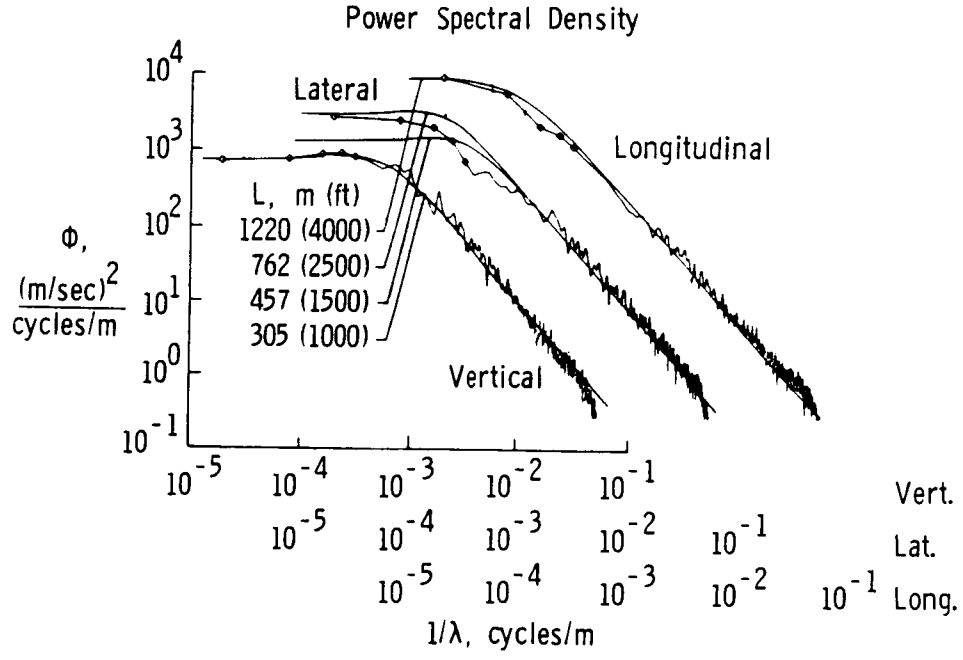

(b) Power spectral density.

Figure 5. Convective case.

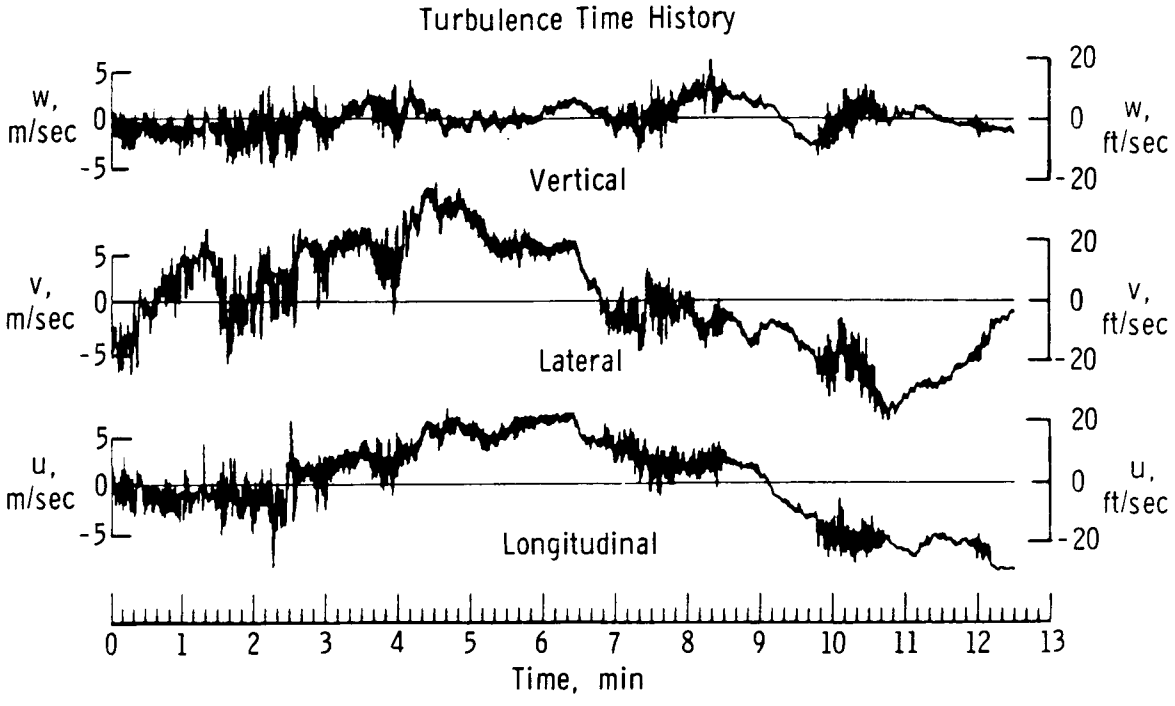

(a) Turbulence time history.

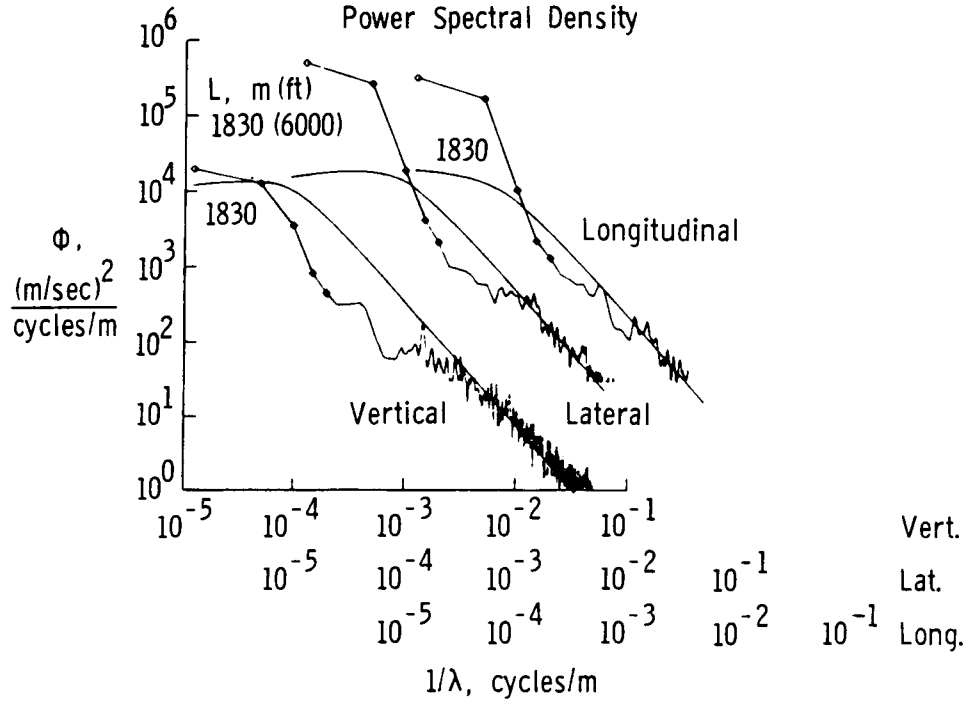

(b) Power spectral density.

Figure 6. Mountain wave case.

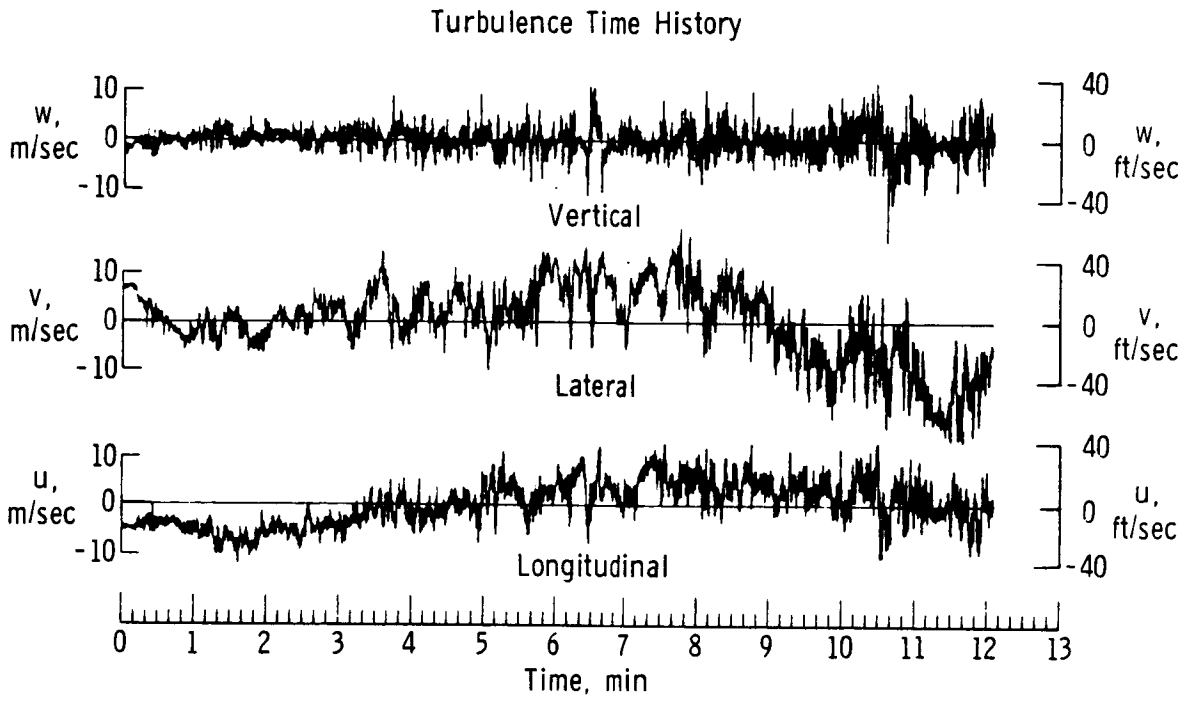

(a) Turbulence time history.

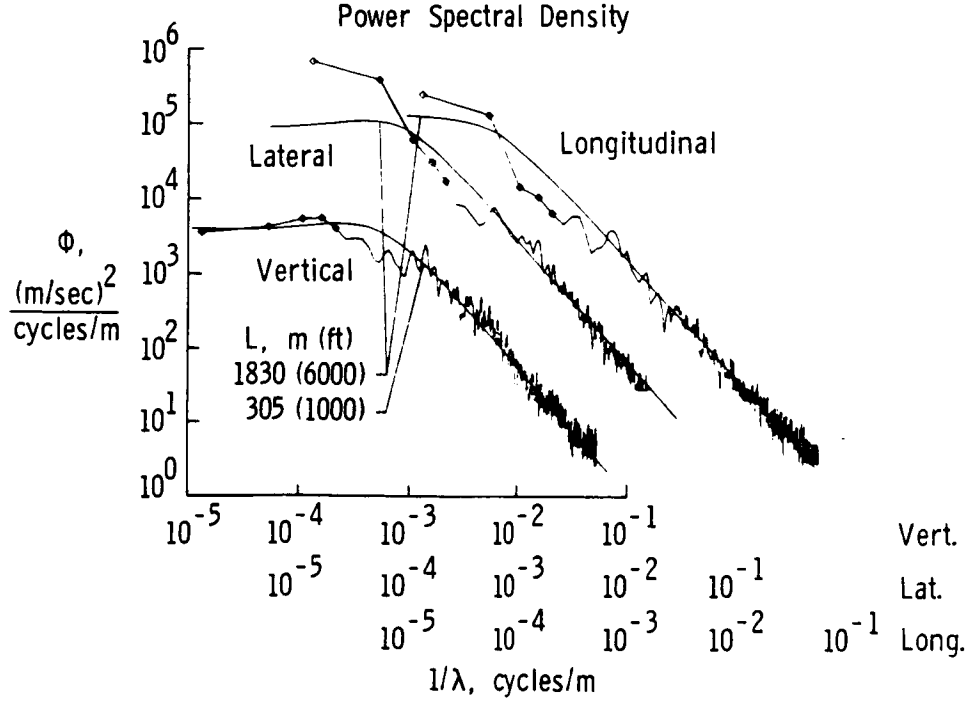

(b) Power spectral density.

Figure 7. High-altitude wind shear case.

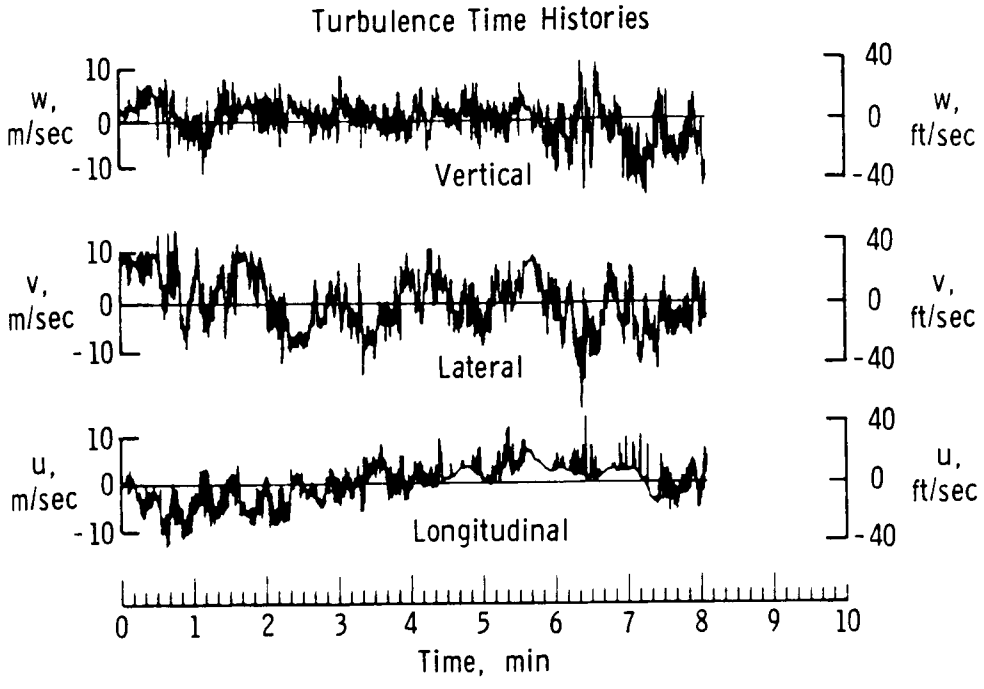

(a) Turbulence time histories.

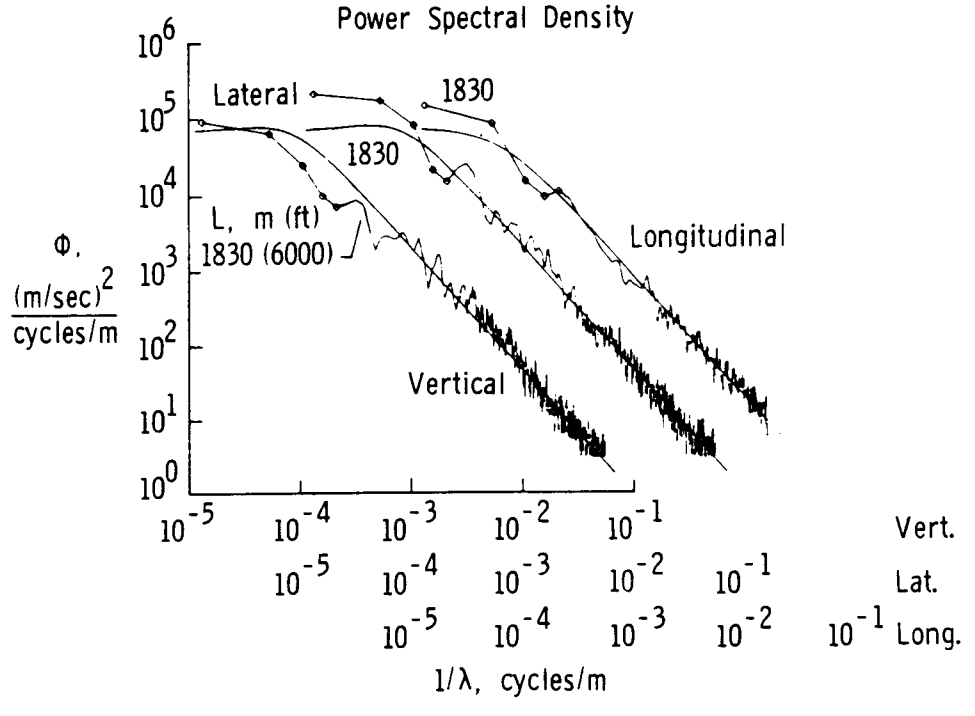

(b) Power spectral density.

Figure 8. Rotor case.

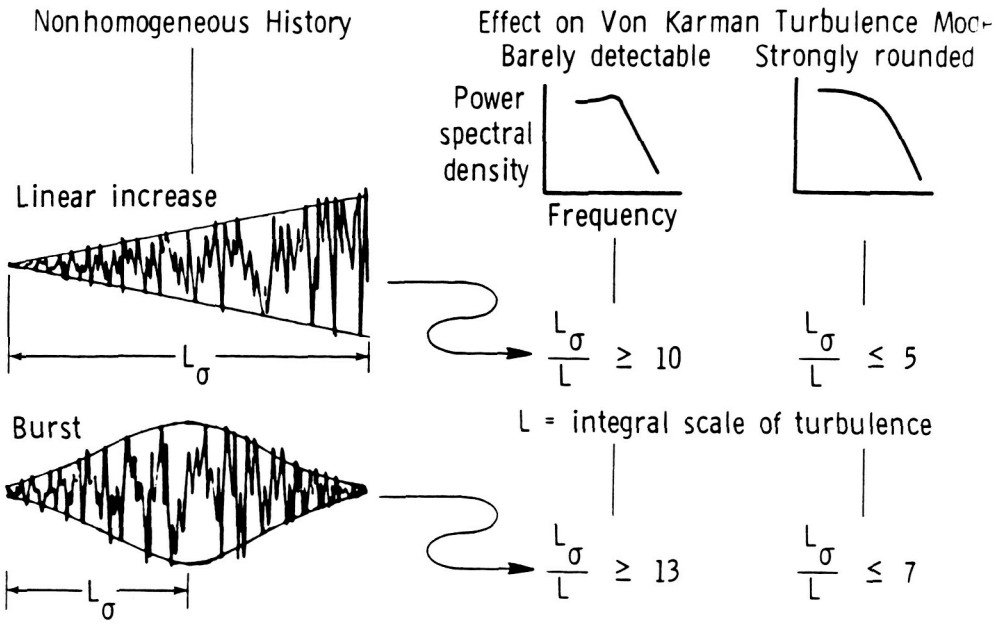

Figure 9. Effects of nonhomogeneous behavior on the power spectra of atmospheric turbulence.

- For wavelengths shorter than approx. 3000 ft , spectrum with - 5/3 slope is reasonable
- For wavelengths greater than 3000 ft , appropriate integral scale value is variable
- In general, vertical component L smaller than that for lateral and longitudinal components

$$L_{vert} \cong 1000 \text{ ft}$$

$$L_{long,\ lat} \cong 6000 \text{ ft}$$

- Mountain wave cases not continuous: spectral representation questionable

Figure 10. Assessment of integral scale value (L).

Objective: Acquisition of in situ atmospheric turbulence data for correlation with analytical models, for use in simulations, and for comparison with data obtained from remote sensing techniques.

- Measure spanwise gust gradients applicable to terminal area operations
- Characterize wind shear, severe strom outflows and low altitude turbulence in utilitarian terms

Figure 11. Spanwise gradient (SPAN-MAT) research.

Figure 12. Test bed airplane.

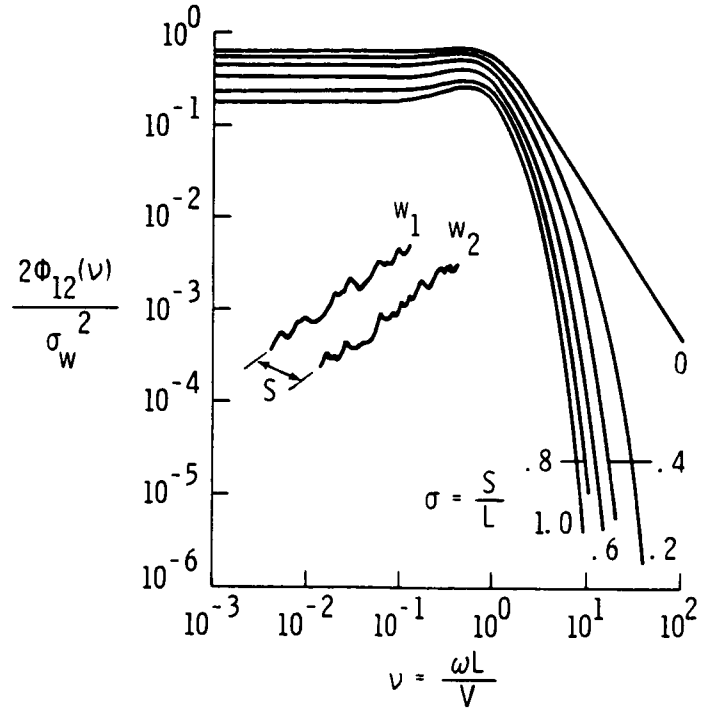

Figure 13. Cross-spectra for treatment of nonuniform spanwise gusts.

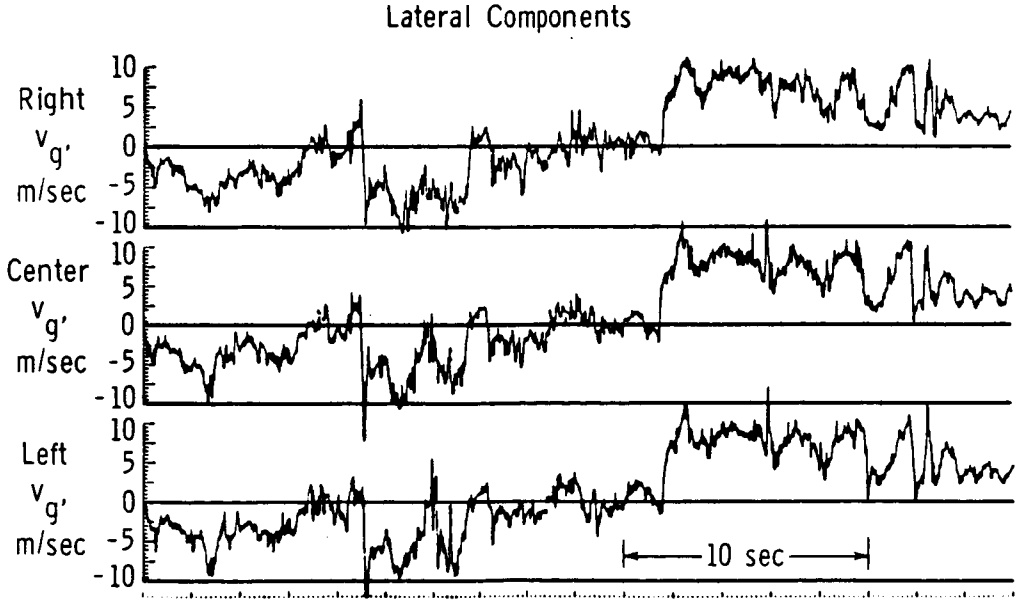

Figure 14.- SPAN-MAT gust velocity time histories.

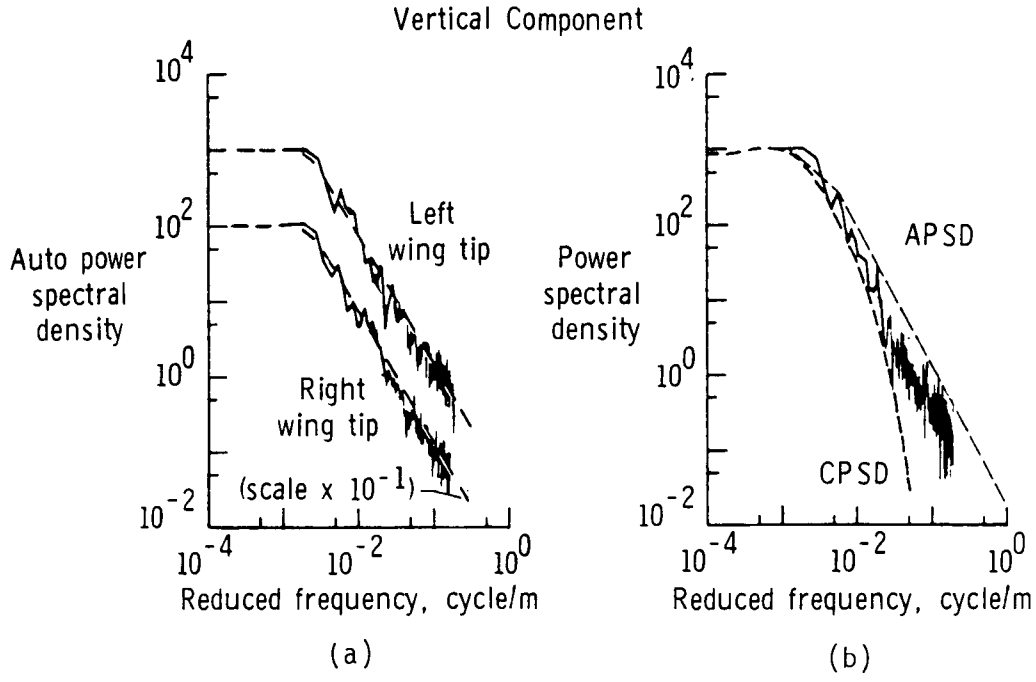

Figure 15. Gust velocity power spectra.

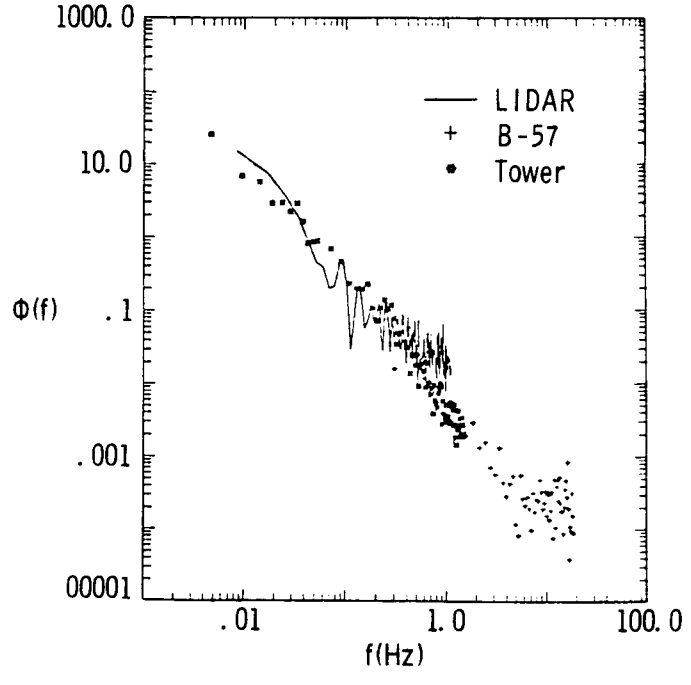

Figure 16. Comparison of ground-based and in situ measurements.

- On-board recorders provide time history records of indicated airspeed, pressure altitude, and normal acceleration
- Derived gust velocity, U_{DE}, computed for acceleration peaks
  - U_{DE} = f(normal accel., equivalent airspeed, lift curve slope, weight, wing area, and gust alleviation factor)
- Recorders installed on numerous transport aircraft beginning in 1950's
  - Program terminated in early 1970's
  - Last report published 1977 on comparison of wide and narrow body long-haul turbine-powered transports
- General aviation program 1960-1982
  - Operation types included single- and twin-executive, personal, instructional, aerial applic., forest fighting, pipeline patrol, commercial fish-spotting, aerobatic, commuter, and float
  - Total of 42,155 hours of data collected from 105 airplanes

Figure 17. NASA VGH program.

- Feasibility of utilizing data available from transport crash recorders demonstrated
  - Data includes normal and lateral c.g. accel., indicated airspeed, pressure altitude, trailing edge flap and spoiler/drag brake position, and autopilot status
  - Data from wide body transports have been edited, processed and compiled (total of 2341 flights and 5067 hours flight time)
- Smart recorder
  - Instrument developed capable of recording, storing, and providing specified flight and ground data in desired format (statistical or time history)

Figure 18. Digital velocity, vertical acceleration in g's, and pressure altitude.

- Detailed analysis of encounters based on flight data recorders
  - Convert response data to atmospheric description
  - Correlation with meteorological phenomena
  - Establish model and install on simulator
  - Study response of different aircraft
- Study to data indicates that:
  - Strong shear layers destablished by storm passage or mountain waves provide disturbance
  - Turbulence is not of random nature, but of periodic large vortex flow

Figure 19. Special clear-air turbulence encounters by commercial airliners.

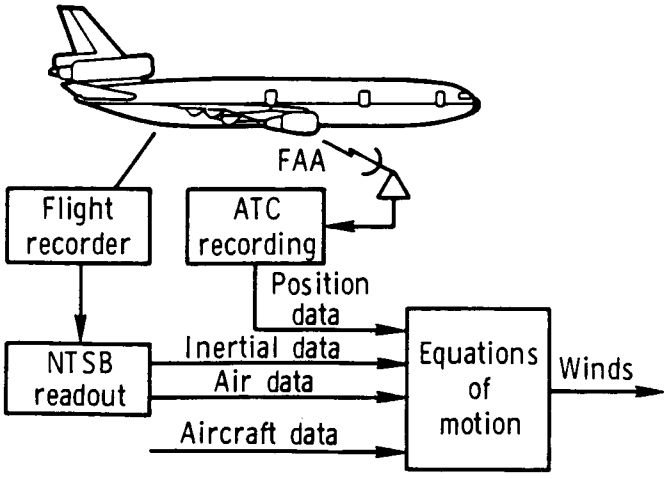

- Eight cases available for analysis
  - All at altitudes between 33000 and 41000 ft
  - Occurrences in 1975, 1981, 1982, 1983(2) and 1985(3)
  - Locations from California to Greenland

Figure 20. Wide body airline accidents/incidents involving atmospheric disturbances at cruise altitudes.